

A New Procedure for the Photometric Parallax Estimation

S. Karaali¹, Y. Karataş,¹ S. Bilir,¹ S. G. Ak¹ and E. Hamzaoğlu²

¹ Department of Astronomy and Space Sciences, Science Faculty, Istanbul University, 34452 Istanbul, Turkey
karsa@istanbul.edu.tr

² Faculty of Engineering and Design, Istanbul Commerce University, 34378 Istanbul, Turkey

Received 2003 March 20, accepted 2003 June 19

Abstract: We present a new procedure for photometric parallax estimation. The data for 1236 stars provide calibrations between the absolute magnitude offset from the Hyades main-sequence and the ultraviolet-excess for eight different $(B-V)_0$ colour-index intervals, (0.3 0.4), (0.4 0.5), (0.5 0.6), (0.6 0.7), (0.7 0.8), (0.8 0.9), (0.9 1.0) and (1.0 1.1). The mean difference between the original and estimated absolute magnitudes and the corresponding standard deviation are rather small, +0.0002 and ± 0.0613 mag. The procedure has been adapted to the Sloan photometry by means of colour equations and applied to a set of artificial stars with different metallicities. The comparison of the absolute magnitudes estimated by the new procedure and the canonical one indicates that a single colour-magnitude diagram does not supply reliable absolute magnitudes for stars with large range of metallicity.

Keywords: photometric parallax — UVB photometry — Sloan photometry

1 Introduction

Stellar kinematics and metallicity are two primary means to deduce the history of our Galaxy. However, such goals can not be achieved without stellar distances. The distance to a star can be evaluated by trigonometric or photometric parallaxes. Trigonometric parallaxes are only available for nearby stars where Hipparcos (ESA, 1997) is the main supplier for the data. For stars at large distances, the use of photometric parallaxes is unavoidable. In other words the study of the Galactic structure is strictly tied to precise determination of absolute magnitudes.

Different methods can be used for absolute magnitude determination. The method used in the Strömgen's *uvby- β* (Nissen & Schuster 1991) and in the UBV (Laird et al. 1988, hereafter LCL) photometry depends on the absolute magnitude offset from a standard main-sequence. In recent years the derivation of absolute magnitudes has been carried out by means of colour-absolute magnitude diagrams of some specific clusters whose metal abundances are generally adopted as the mean metal abundance of a Galactic population, such as thin, thick disks and halos. The studies of Phleps et al. (2000) and Chen et al. (2001) can be given as examples. A slightly different approach is that of Siegel et al. (2002) where two relations, one for stars with solar-like abundances and another one for the metal-poor stars were derived between M_R and the colour-index $R-I$, where M_R is the absolute magnitude in the R filter of Johnson system. For a star of given metallicity and colour, absolute magnitude can be estimated by linear interpolation of two ridgelines and by means of linear extrapolation beyond the metal-poor ridgeline.

We strongly believe we can contribute to this important topic by modifying the method of LCL and by adapting it to Sloan photometry. LCL used the equation

$$M_V(\text{Hyades}) = 5.64(B-V)_0 + 1.11 \quad (1)$$

for the fiducial main-sequence of Hyades as a standard main-sequence and derived the metallicity-dependent offset

$$\Delta M_V^H = \frac{2.31 - 1.04(B-V)_0}{1.594} \times (-0.6888\delta + 53.14\delta^2 - 97.004\delta^3) \quad (2)$$

LCL state that the calibration is valid for $\delta \leq 0.25$, which is equal to $[\text{Fe}/\text{H}] = -1.75$ dex, according to the Carney (1979) transformation of δ into $[\text{Fe}/\text{H}]$

$$[\text{Fe}/\text{H}] = 0.11 - 2.90\delta - 18.68\delta^2 \quad (3)$$

Moreover, LCL give an equation for direct absolute magnitude derivation for extreme metal-poor stars

$$M_V(B-V) = 4.60(B-V)_0 + 3.46 + 1.67(\delta - 0.25) \quad (4)$$

As these equations reveal, the method of LCL is based on the fact that absolute magnitude (and metallicity) is a function of UV-excess, in addition to colour-index. UV-excess is usually defined as the de-reddened $(U-B)$ colour-index difference between a star and a Hyades star of equal $(B-V)_0$. The U -band is centred at a wavelength where metallicity effect is efficient, hence a star with bright U -magnitude, i.e. a relatively metal-poor star, is absolutely faint relative to a Hyades star of equal $(B-V)_0$.

We considered the possibility of calibrating the absolute magnitude offset from the updated Hyades sequence (derivation given in full in the Accessory Material)

$$M_V(\text{Hyades}) = -1.48739(B-V)_0^2 + 7.70982(B-V)_0 + 0.331195 \quad (1')$$

using only δ for different $(B-V)_0$ colour-indices without any restriction for metallicity. This is the main scope of this work. We will show in the following sections that such an approach provides more precise absolute magnitudes than those of LCL. In Section 2 we present the data used

for calibration and in Section 3 the procedure used for calibration is given. The extension of this procedure to the Sloan photometry is given in Section 4 and in Section 5 a detailed discussion is provided.

2 The Data

The V , $B-V$, $U-B$ and $E(B-V)$ photometric data used in this paper and the star distance d are taken from Ryan (1989). For any star the following reductions have been applied

$$\begin{aligned} (B-V)_0 &= (B-V) - E(B-V) & (5) \\ (U-B)_0 &= (U-B) - 0.72E(B-V) \\ &\quad + 0.05E^2(B-V) \\ M_V &= V - 3.1E(B-V) + 5 - 5 \log d \\ \delta(U-B) &= (U-B)_H - (U-B)_0 \end{aligned}$$

$(U-B)_H$ is the de-reddened $(U-B)$ colour-index of a dwarf star of the Hyades cluster with the same $(B-V)_0$ of the star considered. We indicate with ΔM_V^H the absolute magnitude difference between a star and a Hyades star of equal $(B-V)_0$ and with $\delta_{0.6}$ the normalised UV-excess of the star considered (see Table 1), namely $\delta_{0.6}$ is the de-reddened $(U-B)$ colour-index difference between two stars just quoted and necessary coefficient used here is given by Sandage (1969). This procedure is necessary for the equivalence of UV-excess of two stars of the same metal-abundance, one with any $(B-V)_0$ and another one with $(B-V)_0 = 0.6$, where the latter is adopted as a reference colour-index for this reduction (Sandage, 1969). Contrary to Laird et al. (1988) who gave relations as a function of both colour-index $(B-V)_0$ and $\delta_{0.6}$ (equation 2) we prefer to plot ΔM_V^H as a function of only $\delta_{0.6}$ for different $(B-V)_0$ intervals, $0.3 < (B-V)_0 \leq 0.4$; $0.4 < (B-V)_0 \leq 0.5$; $0.5 < (B-V)_0 \leq 0.6$; $0.6 < (B-V)_0 \leq 0.7$; $0.7 < (B-V)_0 \leq 0.8$; $0.8 < (B-V)_0 \leq 0.9$; $0.9 < (B-V)_0 \leq 1.0$ and $1.0 < (B-V)_0 \leq 1.1$. This approach significantly improves the calibrations with respect to those of LCL, as explained in the following sections.

3 Photometric Parallaxes

3.1 Calibration of Absolute Magnitude as a Function of UV-Excess

We used $\Delta M_V^H = M_V(*) - M_V(H)$ and the $\delta_{0.6}$ data listed in Table S1 for a third-degree polynomial, fitting for each $(B-V)_0$ interval cited in Section 2, where $M_V(H)$ and $M_V(*)$ are the absolute magnitudes of a Hyades star, evaluated by equation (1'), and of a programme star of equal $(B-V)_0$, respectively. Stars are separated into different bins in $\delta_{0.6}$ with range $\Delta\delta_{0.6} = 0.05$ mag in order to take into account all the programme stars and to provide reliable statistics. The number of bins is 6 for the bluest and reddest intervals of $0.3 < (B-V)_0 \leq 0.4$ and $1.0 < (B-V)_0 \leq 1.1$ and lie between 9 and 12 for the other six colour-index intervals. The mean of $\delta_{0.6}$ and ΔM_V^H are evaluated

for each bin except one bin in each interval of $0.7 < (B-V)_0 \leq 0.8$; $0.8 < (B-V)_0 \leq 0.9$; $0.9 < (B-V)_0 \leq 1.0$ and $1.0 < (B-V)_0 \leq 1.1$, which have relatively extreme $\delta_{0.6}$ or ΔM_V^H values. According to this criterion, eight stars were excluded from the analysis (see Table 1). Then ΔM_V^H was plotted versus $\delta_{0.6}$ (Fig. 1) and a third-degree polynomial was fitted for each set of data

$$\Delta M_V^H = a_3\delta_{0.6}^3 + a_2\delta_{0.6}^2 + a_1\delta_{0.6} + a_0 \quad (6)$$

The coefficients, a_i , of this equation are given in Table 2 as a function of $(B-V)_0$. One notices two important points in Figure 1. First, a large scattering between the curves exists and, second, contrary to expectations, neither of the curves converge towards the origin. This means that a star with $\delta_{0.6} = 0$, corresponding to the absolute magnitude of a Hyades star, would have a value for ΔM_V^H different from zero and, hence, a different absolute magnitude from the Hyades star, according to the definition of ΔM_V^H . This is a contradiction. The curves should pass through the origin to avoid this discrepancy. Table 2 shows that all the zero points are larger than $\Delta M_V^H = 0.2$. ΔM_V^H increases from $\Delta M_V^H = 0.24$ for the interval $0.3 < (B-V)_0 \leq 0.4$ to a maximum value of $\Delta M_V^H = 0.35$ in the interval $0.6 < (B-V)_0 \leq 0.7$ and declines to such a lower value as $\Delta M_V^H = 0.29$ for the interval $1.0 < (B-V)_0 \leq 1.1$.

We would like to quote the work of Cameron (1985), who discussed the same relation, i.e. $\Delta M(V)$ versus $\delta_{0.6}$. We fitted a third degree polynomial for his data (Table 2 and Figure 6 in that paper) with a constant term of -0.1663 , which is absolutely equal and almost half of the mean of the constant terms in our work. The work of Cameron (1985) also indicates that $\delta_{0.6} = 0$ does not imply $\Delta M(V) = 0.0$.

3.2 Normalisation of the Hyades Main Sequence

The discrepancy mentioned above can be minimised by normalisation of the Hyades main-sequence. In other words, M_V^H needs to be incremented to limit the constant term in equation (6). Table 3 gives M_V^H as evaluated by equation (1'), and the adopted M_V^H , i.e. $M_V^H(\text{ad}) = M_V^H(\text{ev}) + a_0$, where a_0 is the corresponding zero point in equation (6). The $M_V^H(\text{ad})$ are plotted against the mean $(B-V)_0$ for each interval and the following quadratic equation has been fitted (Figure 2).

$$M_V^H(\text{nor}) = -2.1328(B-V)_0^2 + 8.6803(B-V)_0 + 0.305 \quad (7)$$

This is the normalised colour-magnitude equation for the Hyades main-sequence used in the derivation of photometric parallaxes.

3.3 Final Equations for Photometric Parallaxes

After normalisation, the difference in absolute magnitude between a star and a Hyades star of equal $(B-V)_0$, i.e. $\Delta M_V^H(\text{nor})$ is re-evaluated and used in final equations for photometric parallaxes (see Table S2). The procedure is

Table 1. Normalised UV-excesses ($\delta_{0,6}$) and two sets of absolute magnitude differences ($\langle \Delta M_1 \rangle \equiv \Delta M_V^H$ and $\langle \Delta M_2 \rangle \equiv \Delta M_V^H(\text{nor})$), in different bins for stars in eight $(B-V)_0$ colour index intervals. N is the total number of stars in each bin

$\delta_{0,6}$ -interval	$\langle \delta_{0,6} \rangle$	$\langle \Delta M_1 \rangle$	$\langle \Delta M_2 \rangle$	N	$\delta_{0,6}$ -interval	$\langle \delta_{0,6} \rangle$	$\langle \Delta M_1 \rangle$	$\langle \Delta M_2 \rangle$	N
(a) $0.3 < (B-V)_0 \leq 0.4$					(e) $0.7 < (B-V)_0 \leq 0.8$				
(-0.025 +0.025]	-0.010	0.213	-0.046	1	(-0.200 -0.125]	—	—	—	2
(+0.025 +0.075]	0.045	0.364	0.115	2	(-0.125 -0.075]	-0.089	-0.104	-0.442	8
(+0.175 +0.225]	0.200	0.907	0.660	2	(-0.075 -0.025]	-0.041	0.100	-0.238	11
(+0.225 +0.275]	0.260	1.249	0.992	4	(-0.025 +0.025]	-0.001	0.328	-0.010	34
(+0.275 +0.325]	0.304	1.332	1.081	25	(+0.025 +0.075]	0.052	0.568	0.230	47
(+0.325 +0.375]	0.340	1.384	1.137	11	(+0.075 +0.125]	0.102	0.744	0.405	46
(b) $0.4 < (B-V)_0 \leq 0.5$					(+0.125 +0.175]	0.145	0.923	0.585	30
(-0.125 -0.075]	-0.110	-0.121	-0.393	1	(+0.175 +0.225]	0.196	1.117	0.778	15
(-0.075 -0.025]	-0.030	0.097	-0.197	1	(+0.225 +0.275]	0.247	1.207	0.869	9
(-0.025 +0.025]	0.003	0.290	0.006	6	(+0.275 +0.325]	0.297	1.395	1.057	7
(+0.025 +0.075]	0.055	0.552	0.269	6	(+0.325 +0.375]	0.345	1.491	1.153	8
(+0.075 +0.125]	0.096	0.750	0.469	7	(f) $0.8 < (B-V)_0 \leq 0.9$				
(+0.125 +0.175]	0.159	1.102	0.814	15	(-0.175 -0.125]	-0.154	-0.228	-0.561	5
(+0.175 +0.225]	0.204	1.230	0.947	59	(-0.125 -0.075]	-0.093	0.020	-0.309	14
(+0.225 +0.275]	0.250	1.360	1.078	97	(-0.075 -0.025]	-0.050	0.144	-0.186	22
(+0.275 +0.325]	0.301	1.525	1.224	43	(-0.025 +0.025]	0.000	0.323	-0.009	27
(+0.325 +0.375]	0.339	1.609	1.330	9	(+0.025 +0.075]	0.046	0.450	0.118	26
(+0.375 +0.425]	0.390	1.698	1.435	1	(+0.075 +0.125]	0.103	0.657	0.325	21
(c) $0.5 < (B-V)_0 \leq 0.6$					(+0.125 +0.175]	0.145	0.813	0.482	13
(-0.075 -0.025]	-0.060	-0.016	-0.327	2	(+0.175 +0.225]	0.200	0.947	0.617	5
(-0.025 +0.025]	0.015	0.394	0.077	2	(+0.225 +0.275]	0.255	1.201	0.867	8
(+0.025 +0.075]	0.053	0.633	0.317	11	(+0.275 +0.325]	0.299	1.261	0.929	8
(+0.075 +0.125]	0.104	0.826	0.507	35	(+0.325 +0.375]	0.345	1.482	1.148	4
(+0.125 +0.175]	0.153	1.057	0.743	55	(+0.375 +0.425]	0.398	1.525	1.196	4
(+0.175 +0.225]	0.202	1.240	0.928	67	(+0.425 +0.600]	—	—	—	4
(+0.225 +0.275]	0.250	1.440	1.129	71	(g) $0.9 < (B-V)_0 \leq 1.0$				
(+0.275 +0.325]	0.292	1.588	1.275	24	(-0.075 -0.025]	-0.055	0.226	-0.081	2
(+0.325 +0.375]	0.337	1.740	1.429	3	(-0.025 +0.025]	0.004	0.334	0.017	5
(d) $0.6 < (B-V)_0 \leq 0.7$					(+0.025 +0.075]	0.058	0.452	0.137	12
(-0.175 -0.075]	-0.153	-0.393	-0.726	3	(+0.075 +0.125]	0.105	0.585	0.272	15
(-0.075 -0.025]	-0.028	0.215	-0.119	6	(+0.125 +0.175]	0.151	0.706	0.392	11
(-0.025 +0.025]	0.013	0.439	0.104	11	(+0.175 +0.225]	0.198	0.811	0.498	4
(+0.025 +0.075]	0.052	0.593	0.261	26	(+0.275 +0.325]	0.300	—	—	1
(+0.075 +0.125]	0.102	0.834	0.502	51	(h) $1.0 < (B-V)_0 \leq 1.1$				
(+0.125 +0.175]	0.150	1.052	0.720	61	(-0.325 -0.275]	—	—	—	1
(+0.175 +0.225]	0.202	1.240	0.907	39	(+0.025 +0.075]	0.040	0.336	0.047	1
(+0.225 +0.275]	0.250	1.416	1.085	26	(+0.075 +0.125]	0.107	0.478	0.195	6
(+0.275 +0.325]	0.297	1.560	1.230	10	(+0.125 +0.175]	0.130	0.489	0.204	1
(+0.325 +0.425]	0.353	1.571	1.239	3	(+0.175 +0.225]	0.199	0.600	0.323	7
					(+0.225 +0.275]	0.237	0.754	0.469	3
					(+0.275 +0.325]	0.310	0.853	0.572	1

the same as in Section 3.1. The mean of $\Delta M_V^H(\text{nor})$ for each bin is given in the fourth column of Table 1. The plot of $\Delta M_V^H(\text{nor})$ against $\delta_{0,6}$ for each $(B-V)_0$ interval yields the following third-degree polynomial

$$\Delta M_V^H(\text{nor}) = b_3 \delta_{0,6}^3 + b_2 \delta_{0,6}^2 + b_1 \delta_{0,6} + b_0 \quad (8)$$

The coefficients, b_i , of this equation are given in Table 4 and the plots are shown in Figure 3. The curves in Figure 3

exhibit a different appearance than the corresponding ones in Figure 1. The dispersion of the curves in Figure 3 is smaller and now all the curves pass almost through the origin (see the term b_0 in Table 4). We used equation (8) to evaluate $\Delta M_V^H(\text{nor})$ for all the programme stars and to estimate $M_V^H(\text{est})$ by the definition of the offset, i.e. $\Delta M_V^H(\text{nor}) = M_V^H(\text{est}) - M_V^H(\text{nor})$. Surprisingly, the differences between the estimated and original absolute magnitudes ΔM_V^H are rather small. The mean of these differences for each $(B-V)_0$ -interval is almost zero

Table 2. Numerical values for the coefficients in equation (6) as a function of $(B-V)_0$ colour-index

$(B-V)_0$	a_3	a_2	a_1	a_0
(0.3 0.4]	-35.7800	+17.9170	+1.4505	+0.2389
(0.4 0.5]	-15.4620	+3.5129	+4.5340	+0.2865
(0.5 0.6]	+4.9011	-5.3226	+5.4334	+0.3294
(0.6 0.7]	-11.0040	-0.3570	+5.0207	+0.3491
(0.7 0.8]	+0.0737	-3.6154	+4.6223	+0.3237
(0.8 0.9]	-2.4661	+0.1822	+3.4514	+0.3102
(0.9 1.0]	-20.8350	+6.0860	+2.0942	+0.3206
(1.0 1.1]	-8.3965	+5.0002	+1.0912	+0.2903

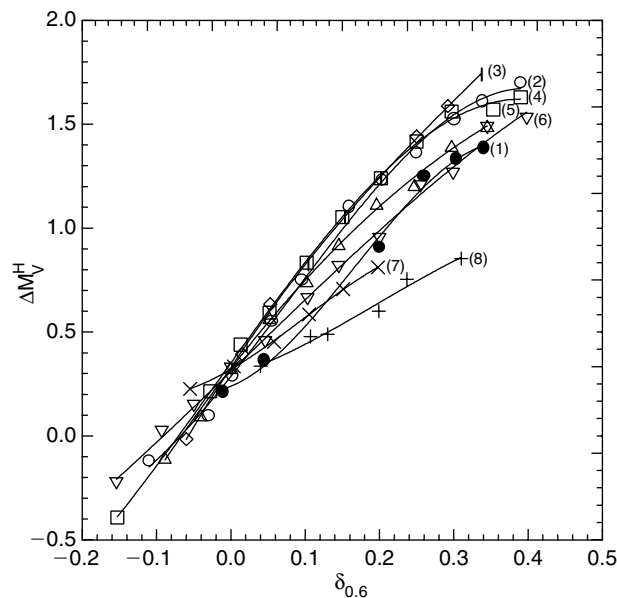


Figure 1 ΔM_V^H versus $\delta_{0.6}$ for eight $(B-V)_0$ colour-index intervals. The symbols are (●): $0.3 < (B-V)_0 \leq 0.4$; (○): $0.4 < (B-V)_0 \leq 0.5$; (◇): $0.5 < (B-V)_0 \leq 0.6$; (□): $0.6 < (B-V)_0 \leq 0.7$; (△): $0.7 < (B-V)_0 \leq 0.8$; (▽): $0.8 < (B-V)_0 \leq 0.9$; (×): $0.9 < (B-V)_0 \leq 1.0$; and (+): $1.0 < (B-V)_0 \leq 1.1$.

Table 3. Two sets of absolute magnitudes for the Hyades cluster as a function of $(B-V)_0$ colour-index. M_V^H evaluated by equation (1') and M_V^H (ad) adopted for normalisation

$(B-V)_0$	$\langle (B-V)_0 \rangle$	M_V^H	M_V^H (ad)
(0.3 0.4]	0.384	3.07	3.31
(0.4 0.5]	0.458	3.55	3.84
(0.5 0.6]	0.557	4.16	4.49
(0.6 0.7]	0.655	4.74	5.09
(0.7 0.8]	0.751	5.28	5.61
(0.8 0.9]	0.854	5.83	6.14
(0.9 1.0]	0.945	6.29	6.61
(1.0 1.1]	1.045	6.76	7.05

and their standard deviations are only few percent. However, this is not the result for the procedure applied by LCL (Table 5 and Figure 4; see Section 5 for detailed discussion).

The evolutionary effect has not been considered above. However, the $(U-B)_0$ versus $(B-V)_0$ sequence slightly

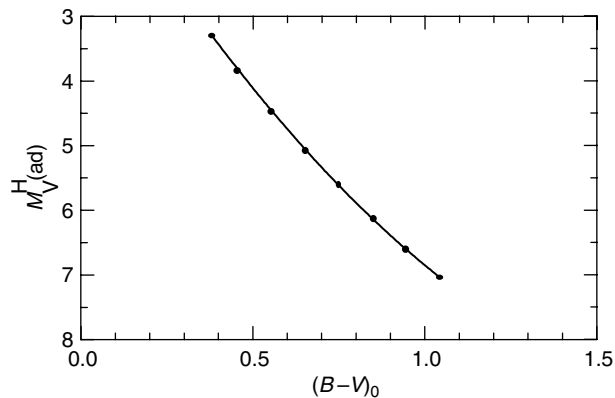


Figure 2 Adopted absolute magnitudes for the Hyades main-sequence versus $(B-V)_0$ colour-index.

Table 4. Numerical values for the coefficients of equation (8) as a function of $(B-V)_0$ colour-index

$(B-V)_0$	b_3	b_2	b_1	b_0
(0.3 0.4]	-32.1800	+15.9370	+1.7350	-0.0177
(0.4 0.5]	-15.3820	+3.7188	+4.4850	+0.0022
(0.5 0.6]	+3.9109	-4.8075	+5.3847	+0.0134
(0.6 0.7]	-11.1700	-0.3015	+5.0281	+0.0153
(0.7 0.8]	+0.1049	-3.6157	+4.6196	-0.0144
(0.8 0.9]	-22.5350	+0.1109	+3.4469	-0.0203
(0.9 1.0]	-24.9710	+7.2916	+2.0269	+0.0051
(1.0 1.1]	-7.4029	+4.2761	+1.2638	-0.0047

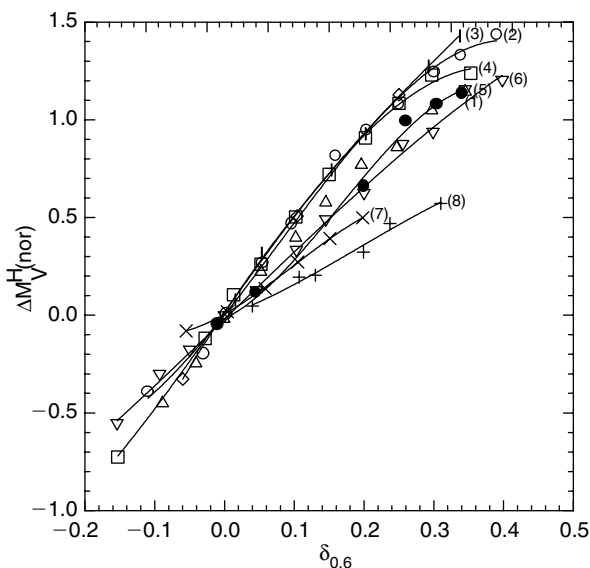


Figure 3 ΔM_V^H (nor) versus $\delta_{0.6}$ for eight $(B-V)_0$ colour-index intervals (symbols as in Figure 1).

varies as a function of the gravity. Therefore for stars close to the end of the main sequence (TAMS), the estimate of real $\delta_{0.6}$ is smaller. We used the Yale isochrones of Yi et al. (2001) for the following chemical composition and checked the size of the errors introduced by evolutionary effects between the zero age main-sequence (ZAMS) and TAMS (10 Gyr): $Y=0.27$ and $Z=0.02$

([Fe/H] = +0.05 dex). For this sample, $\langle \delta_{0,6} \rangle = 0.0$ and 0.02 for $0.81 < (B-V)_0 \leq 1.00$ and $0.7 < (B-V)_0 \leq 0.81$, respectively. The effect of the difference in $\Delta M_V^H(\text{nor})$ for a star with $\delta_{0,6} = 0.2$ ([Fe/H] = -1.2 dex) is 8%.

4 Extension of the Procedure to the Sloan Photometry

4.1 Transformation of the Normalised UV-Excess from UBV to the Sloan Photometry and New Metallicity Calibration

The following colour equations of Fukugita et al. (1996) provide a relation between the normalised UV-excesses

for UBV and Sloan photometries, and the new metallicity calibration for the Sloan photometric system

$$(g'-r')_0 = 1.05(B-V)_0 - 0.23 \tag{9a}$$

$$(u'-g')_0 = 1.38(U-B)_0 + 1.14 \tag{9b}$$

Let us write equation (9b) for two stars with the same $(B-V)_0$ (or equivalently $(g'-r')_0$), i.e. for a Hyades star (H) and for a star (*) whose UV-excess is normalised to

$$(u'-g')_H = 1.38(U-B)_H + 1.14 \tag{10}$$

$$(u'-g')_* = 1.38(U-B)_* + 1.14$$

Then, the UV-excess for the star in question, relative to the Hyades star is

$$(u'-g')_H - (u'-g')_* = 1.38[(U-B)_H - (U-B)_*] \tag{11}$$

or, in standard notation

$$\delta(u'-g') = 1.38\delta(U-B) \tag{12}$$

If we apply this equation to a star with $(B-V)_0 = 0.6$, corresponding to $(g'-r')_0 = 0.4$, we obtain

$$\delta(u'-g')_{0.4} = 1.38\delta(U-B)_{0.6} \tag{13}$$

for the relation between the normalised UV-excesses in the UBV and the Sloan systems. From this equation

Table 5. The mean difference between the original absolute magnitudes and the absolute magnitudes estimated by two different procedures and the corresponding standard deviations

$(B-V)_0$	$\langle M_V(\text{ori}) - M_V(\text{est}) \rangle$		σ	
	New procedure	LCL	New procedure	LCL
(0.3 0.4]	+0.003	-0.845	± 0.087	± 0.272
(0.4 0.5]	-0.009	-0.601	0.070	0.439
(0.5 0.6]	+0.001	-0.100	0.056	0.291
(0.6 0.7]	-0.004	+0.161	0.064	0.304
(0.7 0.8]	+0.003	+0.200	0.062	0.250
(0.8 0.9]	0.000	+0.173	0.053	0.313
(0.9 1.0]	0.000	+0.048	0.034	0.197
(1.0 1.1]	-0.001	-0.385	0.063	0.288

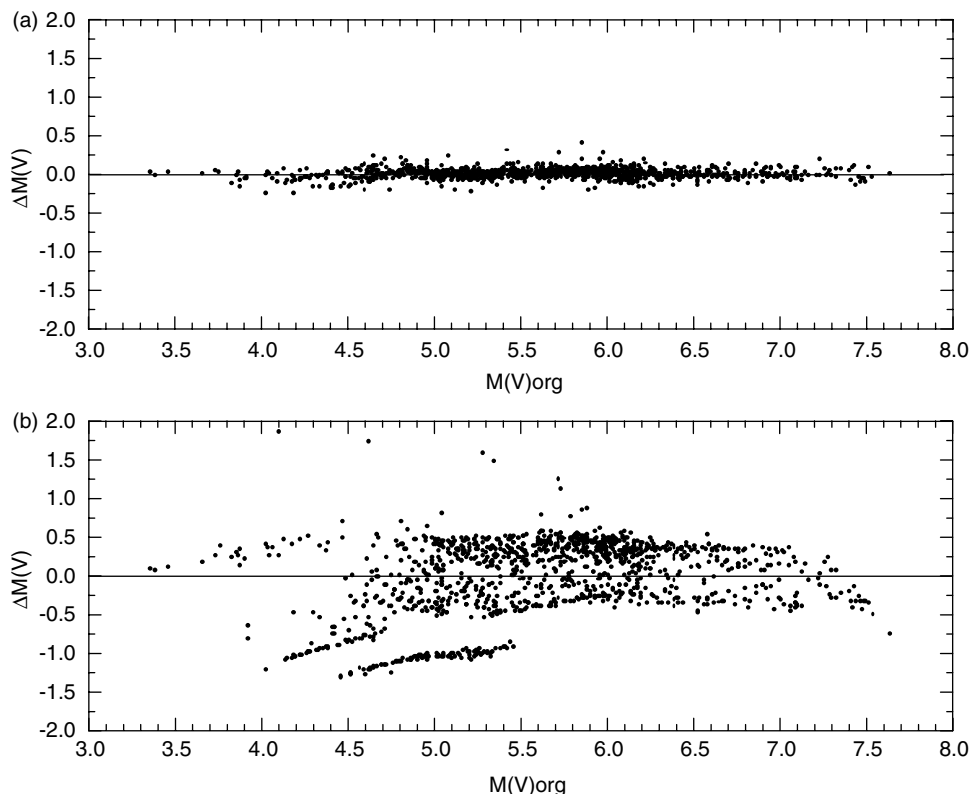


Figure 4 Deviation of the evaluated absolute magnitudes relative to the original absolute magnitudes for (a) the new procedure and (b) LCL.

we obtain

$$\delta(U-B)_{0.6} = 0.725\delta(u'-g')_{0.4} \quad (14)$$

which yields a new metallicity calibration for the Sloan photometry by its substitution in

$$[\text{Fe}/\text{H}] = 0.10 - 2.76\delta_{0.6} - 24.04\delta_{0.6}^2 + 30.00\delta_{0.6}^3 \quad (15)$$

which covers a large range of metallicity, i.e. $-2.75 \leq [\text{Fe}/\text{H}] \leq 0.2$ dex (Karaali et al., 2003). Hence, the new metallicity calibration for the Sloan photometry is obtained as follows

$$[\text{Fe}/\text{H}] = 0.10 - 2.00\delta_{0.4} - 12.64\delta_{0.4}^2 + 11.43\delta_{0.4}^3 \quad (16)$$

Finally, we can show that the coefficients given by Sandage (1969) for the UBV photometry can also be used for the normalisation of the UV-excesses in the Sloan photometry. Take another star with any $B-V$ (or equivalent $g'-r'$) but with the same metallicity as the first star. The relation between its normalised UV-excesses in the two systems would be as equation (12). Hence, from (12) and (13) we obtain

$$\delta(u'-g')_{0.4}/\delta(u'-g') = \delta(U-B)_{0.6}/\delta(U-B) = f \quad (17)$$

where f is the UV-excess normalised factor.

4.2 Photometric Parallaxes for the Sloan Photometry

As mentioned above, the procedure in Section 3.3 can be adopted for photometric parallax derivation also for the Sloan photometry by using the colour equations and the relation between the normalised UV-excesses in two systems. First, we draw $(B-V)_0$ from equation (9a)

$$(B-V)_0 = 0.952(g'-r')_0 + 0.219 \quad (18)$$

and then substitute it into (7) for normalisation of the Hyades main-sequence in the Sloan photometry as follows

$$M_{g'}^{\text{H}}(\text{nor}) = -1.9330(g'-r')_0^2 + 7.3742(g'-r')_0 + 2.1036 \quad (19)$$

Bearing in mind that the offsets from the fiducial sequence of Hyades in two systems are equal, the offset for Sloan photometry can be derived by replacing the equivalence of $\delta(U-B)_{0.6}$ in equation (14) into (8). The following result is obtained:

$$\Delta M_{g'}^{\text{H}}(\text{nor}) = c_3\delta_{0.4}^3 + c_2\delta_{0.4}^2 + c_1\delta_{0.4} + c_0 \quad (20)$$

where the coefficients c_i are given in Table 6 as a function of $(g'-r')_0$.

4.3 Comparison of the Absolute Magnitudes Derived by the New Procedure and the Colour-Magnitude Diagram of a Specific Cluster

As an example, we compared the absolute magnitudes derived by the new procedure and the colour-magnitude diagram of cluster M13 used for the photometric parallax estimation for halo dwarfs (cf. Chen et al. 2001). One

Table 6. Numerical values for the coefficients in equation (20) as a function of $(g'-r')_0$ colour-index. The colour-index intervals correspond to the $(B-V)_0$ intervals in the first columns of Tables 2 and 4

$(g'-r')_0$	c_3	c_2	c_1	c_0
(0.09 0.19]	-12.2631	+8.3769	+1.2579	-0.0177
(0.19 0.30]	-5.8617	+1.9547	+3.2516	+0.0022
(0.30 0.40]	+1.4904	-2.5269	+3.9039	+0.0134
(0.40 0.51]	-4.2566	-0.1585	+3.6454	+0.0153
(0.51 0.61]	+0.0400	-1.9005	+3.3492	-0.0144
(0.61 0.72]	-0.8588	+0.0583	+2.4990	-0.0203
(0.72 0.82]	-9.5159	+3.8326	+1.4695	+0.0051
(0.82 0.93]	-2.8210	+2.2476	+0.9163	-0.0047

Table 7. Colour-magnitude diagram for M13 in UBV and Sloan systems

$(B-V)_0$	M_V	$(g'-r')_0$	$M_{g'}$
0.407	3.70	0.197	3.808
0.410	3.90	0.201	4.010
0.410	4.10	0.201	4.210
0.419	4.30	0.210	4.415
0.414	4.50	0.205	4.612
0.440	4.70	0.232	4.826
0.448	4.90	0.240	5.031
0.500	5.10	0.295	5.260
0.501	5.30	0.296	5.461
0.531	5.50	0.328	5.677
0.550	5.70	0.348	5.888
0.587	5.90	0.386	6.109
0.642	6.10	0.444	6.340
0.682	6.30	0.486	6.562
0.713	6.50	0.519	6.779
0.784	6.70	0.593	7.019
0.821	6.90	0.632	7.240
0.864	7.10	0.677	7.464
0.918	7.30	0.734	7.694
0.945	7.50	0.762	7.909
1.110	7.70	0.936	8.202

can extend this comparison to the other components of the Galaxy. The work is carried out as follows. First, we used the UBV data of Richer & Fahlman (1986) and evaluated the $(g'-r')_0$ and the $M_{g'}$ absolute magnitudes for the main-sequence of M13 via equation (9a) and the following colour equation, which is adopted from Fukugita et al. (1996)

$$M_{g'} = M(V) + 0.56(B-V)_0 - 0.12 \quad (21)$$

The $(g'-r')_0$ and $M_{g'}$ data thus obtained (Table 7) transform the main-sequence of cluster M13 from UBV to the Sloan photometry

$$M'_{g'}(\text{M13}) = 11.442(g'-r')_0^3 - 25.292(g'-r')_0^2 + 21.599(g'-r')_0 + 0.8621 \quad (22)$$

Equation (22) yields direct absolute magnitude estimates for metal-poor stars such as halo dwarfs.

As a second step, we adopted seven sample of artificial stars with $(g'-r')_0$ between 0.20 and 0.50 but with different metallicities, and evaluated their absolute magnitudes by using equation (19) and the related one in (20). The selection of this colour-index interval is due to the work of Chen et al. (2001). These authors assumed that stars fainter than $g' \sim 18$ mag with $0.20 \leq (g'-r')_0 \leq 0.50$ belong to the halo population and used the colour-magnitude diagram of cluster M13, without any metallicity restriction, for their absolute magnitude determination. However, we adopted different metallicities for different samples to reveal the difference between two procedures. As it is easier to derive the metallicity from the normalised UV-excess, we adopted $\delta_{0.4} = 0.00, 0.10, 0.20, 0.30, 0.40, 0.50$ and 0.60 respectively which correspond to the metallicities $[\text{Fe}/\text{H}] = 0.10, -0.21, -0.71, -1.33, -1.99, -2.63$ and -3.18 dex. Table 8 gives the full set of $(g'-r')_0$ cited, the corresponding $M_{g'}^{\text{H}}(\text{nor})$, the $\Delta M_{g'}^{\text{H}}(\text{nor})$ and $M_{g'}$.

Finally, we evaluated another set of $M_{g'}$, by means of equation (22) and compared them with the $M_{g'}$ in the seven sets mentioned above (Table 9). The mean of the differences between the $M_{g'}$ derived by the new procedure and those evaluated by means of equation (22)

i.e.: $\langle \Delta M \rangle \equiv M_{g'}(M13) - M_{g'}(\delta_{0.4})$ are larger for relatively metal-rich stars as expected and least for $[\text{Fe}/\text{H}] \approx -2$ dex. The following third-degree polynomial is a good fit to the couple $\langle \Delta M \rangle$ and $\delta_{0.4}$ (Figure 5)

$$\delta_{0.4} = -0.2305 \langle \Delta M \rangle^3 + 0.5374 \langle \Delta M \rangle^2 - 0.6575 \langle \Delta M \rangle + 0.4369 \quad (23)$$

Equation (23) also reveals that $\langle \Delta M \rangle = 0$ for $\delta_{0.4} = 0.4369$ or $[\text{Fe}/\text{H}] = -2.23$ dex. This result indicates that a colour-magnitude diagram with metallicity less than the one for M13 ($[\text{Fe}/\text{H}] \approx -1.4$ dex) is more appropriate for the photometric parallax estimation for metal-poor stars in deep surveys such as SDSS (as explained in the discussion).

5 Discussion

We have used the high-precision UBV data of Ryan (1989) for absolute magnitude estimation. Although LCL already derived two equations, one for stars with metallicity $[\text{Fe}/\text{H}] \geq -1.75$ dex and another for extreme metal poor stars (equations 2 and 4 respectively), both equations are functions of $(B-V)_0$ and of the normalised $\delta_{0.6}$

Table 8. Absolute magnitudes for a set of artificial stars of different metallicities with $0.2 \leq (g'-r')_0 \leq 0.5$. The columns are (1) $(g'-r')_0$ colour-index; (2) normalised absolute magnitude for a Hyades star of this colour-index; (3)–(9) and (10)–(16) absolute magnitude differences ($\Delta M_{g'}^{\text{H}}(\text{nor})$) and absolute magnitudes $M_{g'}$ evaluated for $\delta_{0.4} = 0.0, 0.1, 0.2, 0.3, 0.4, 0.5$ and 0.6 respectively

1	2	3	4	5	6	7	8	9	10	11	12	13	14	15	16
0.20	3.501	0.0022	0.341	0.684	0.995	1.240	1.384	1.391	3.483	3.842	4.185	4.496	4.742	4.885	4.892
0.21	3.567	0.0022	0.341	0.684	0.995	1.240	1.384	1.391	3.549	3.908	4.251	4.562	4.807	4.951	4.958
0.22	3.632	0.0022	0.341	0.684	0.995	1.240	1.384	1.391	3.615	3.973	4.316	4.628	4.873	5.016	5.023
0.23	3.697	0.0022	0.341	0.684	0.995	1.240	1.384	1.391	3.680	4.038	4.381	4.693	4.938	5.081	5.088
0.24	3.762	0.0022	0.341	0.684	0.995	1.240	1.384	1.391	3.744	4.103	4.446	4.757	5.003	5.146	5.153
0.25	3.826	0.0022	0.341	0.684	0.995	1.240	1.384	1.391	3.809	4.167	4.510	4.822	5.067	5.210	5.217
0.26	3.890	0.0022	0.341	0.684	0.995	1.240	1.384	1.391	3.873	4.231	4.574	4.886	5.131	5.274	5.281
0.27	3.954	0.0022	0.341	0.684	0.995	1.240	1.384	1.391	3.936	4.295	4.638	4.949	5.194	5.338	5.344
0.28	4.017	0.0022	0.341	0.684	0.995	1.240	1.384	1.391	3.999	4.358	4.701	5.012	5.257	5.401	5.408
0.29	4.080	0.0022	0.341	0.684	0.995	1.240	1.384	1.391	4.062	4.421	4.763	5.075	5.320	5.464	5.470
0.30	4.142	0.0022	0.341	0.684	0.995	1.240	1.384	1.391	4.124	4.483	4.826	5.137	5.382	5.526	5.533
0.31	4.204	0.0134	0.380	0.705	0.997	1.266	1.520	1.767	4.217	4.584	4.909	5.201	5.470	5.724	5.970
0.32	4.265	0.0134	0.380	0.705	0.997	1.266	1.520	1.767	4.279	4.645	4.970	5.263	5.531	5.785	6.032
0.33	4.327	0.0134	0.380	0.705	0.997	1.266	1.520	1.767	4.340	4.707	5.032	5.324	5.593	5.847	6.093
0.34	4.387	0.0134	0.380	0.705	0.997	1.266	1.520	1.767	4.401	4.767	5.092	5.385	5.653	5.907	6.154
0.35	4.448	0.0134	0.380	0.705	0.997	1.266	1.520	1.767	4.461	4.828	5.153	5.445	5.714	5.968	6.214
0.36	4.508	0.0134	0.380	0.705	0.997	1.266	1.520	1.767	4.521	4.888	5.213	5.505	5.774	6.028	6.274
0.37	4.567	0.0134	0.380	0.705	0.997	1.266	1.520	1.767	4.581	4.947	5.272	5.565	5.833	6.087	6.334
0.38	4.627	0.0134	0.380	0.705	0.997	1.266	1.520	1.767	4.640	5.007	5.332	5.624	5.893	6.147	6.393
0.39	4.686	0.0134	0.380	0.705	0.997	1.266	1.520	1.767	4.699	5.066	5.391	5.683	5.952	6.205	6.452
0.40	4.744	0.0134	0.380	0.705	0.997	1.266	1.520	1.767	4.757	5.124	5.449	5.741	6.010	6.264	6.511
0.41	4.802	0.0153	0.374	0.704	0.980	1.176	1.266	1.224	4.817	5.176	5.506	5.782	5.978	6.068	6.026
0.42	4.860	0.0153	0.374	0.704	0.980	1.176	1.266	1.224	4.875	5.234	5.564	5.840	6.035	6.126	6.084
0.43	4.917	0.0153	0.374	0.704	0.980	1.176	1.266	1.224	4.932	5.291	5.621	5.897	6.093	6.183	6.141
0.44	4.974	0.0153	0.374	0.704	0.980	1.176	1.266	1.224	4.989	5.348	5.678	5.954	6.150	6.240	6.198
0.45	5.031	0.0153	0.374	0.704	0.980	1.176	1.266	1.224	5.046	5.405	5.735	6.010	6.206	6.297	6.255
0.46	5.087	0.0153	0.374	0.704	0.980	1.176	1.266	1.224	5.102	5.461	5.791	6.066	6.262	6.353	6.311
0.47	5.142	0.0153	0.374	0.704	0.980	1.176	1.266	1.224	5.158	5.516	5.846	6.122	6.318	6.409	6.366
0.48	5.198	0.0153	0.374	0.704	0.980	1.176	1.266	1.224	5.213	5.572	5.902	6.178	6.374	6.464	6.422
0.49	5.253	0.0153	0.374	0.704	0.980	1.176	1.266	1.224	5.268	5.627	5.957	6.233	6.429	6.519	6.477
0.50	5.307	0.0153	0.374	0.704	0.980	1.176	1.266	1.224	5.323	5.681	6.011	6.287	6.483	6.574	6.531

Table 9. Comparison of the absolute magnitudes estimated by the new procedure and by means of a colour–magnitude diagram for the cluster M13 for the artificial stars in question. The columns are (1) colour index $(g'-r')_0$; (2) absolute magnitude $M_{g'}$ (M13) evaluated by equation (22); (3)–(9) difference between the absolute magnitude $M_{g'}$ (M13) and the absolute magnitudes estimated for $\delta_{0.4} = 0.0$ – 0.6 (columns 10–16, Table 8). The averages of these differences ($\langle \Delta M \rangle$) and the corresponding standard deviations σ are given beneath

1	2	3	4	5	6	7	8	9
0.20	4.260	0.776	0.418	0.075	-0.237	-0.482	-0.625	-0.632
0.21	4.386	0.837	0.478	0.136	-0.176	-0.421	-0.565	-0.571
0.22	4.509	0.895	0.536	0.193	-0.118	-0.363	-0.507	-0.514
0.23	4.629	0.949	0.590	0.248	-0.064	-0.309	-0.453	-0.459
0.24	4.745	1.000	0.642	0.299	-0.013	-0.258	-0.401	-0.408
0.25	4.857	1.049	0.690	0.347	0.036	-0.209	-0.353	-0.360
0.26	4.967	1.094	0.735	0.393	0.081	-0.164	-0.308	-0.314
0.27	5.073	1.137	0.778	0.435	0.124	-0.122	-0.265	-0.272
0.28	5.175	1.176	0.817	0.475	0.163	-0.082	-0.225	-0.232
0.29	5.275	1.213	0.854	0.512	0.200	-0.045	-0.189	-0.195
0.30	5.371	1.247	0.889	0.546	0.234	-0.011	-0.154	-0.161
0.31	5.465	1.248	0.881	0.556	0.264	-0.005	-0.259	-0.505
0.32	5.556	1.277	0.910	0.585	0.293	0.024	-0.230	-0.476
0.33	5.643	1.303	0.937	0.612	0.319	0.051	-0.203	-0.450
0.34	5.728	1.328	0.961	0.636	0.344	0.075	-0.179	-0.426
0.35	5.811	1.349	0.983	0.658	0.365	0.097	-0.157	-0.404
0.36	5.890	1.369	1.002	0.677	0.385	0.116	-0.138	-0.384
0.37	5.967	1.386	1.020	0.695	0.402	0.134	-0.120	-0.367
0.38	6.042	1.402	1.035	0.710	0.418	0.149	-0.105	-0.352
0.39	6.114	1.415	1.048	0.723	0.431	0.162	-0.092	-0.339
0.40	6.183	1.426	1.059	0.734	0.442	0.173	-0.081	-0.327
0.41	6.251	1.433	1.075	0.745	0.469	0.273	0.182	0.225
0.42	6.316	1.441	1.082	0.752	0.476	0.280	0.190	0.232
0.43	6.379	1.446	1.088	0.758	0.482	0.286	0.195	0.238
0.44	6.439	1.450	1.091	0.761	0.486	0.290	0.199	0.241
0.45	6.498	1.452	1.094	0.764	0.488	0.292	0.201	0.244
0.46	6.555	1.453	1.094	0.764	0.489	0.293	0.202	0.244
0.47	6.610	1.452	1.093	0.763	0.488	0.292	0.201	0.243
0.48	6.663	1.450	1.091	0.761	0.485	0.289	0.199	0.241
0.49	6.714	1.446	1.087	0.757	0.482	0.286	0.195	0.237
0.50	6.764	1.441	1.082	0.752	0.477	0.281	0.190	0.232
	$\langle \Delta M \rangle$	1.269	0.908	0.575	0.281	0.044	-0.118	-0.186
	σ	0.205	0.204	0.210	0.224	0.237	0.256	0.313

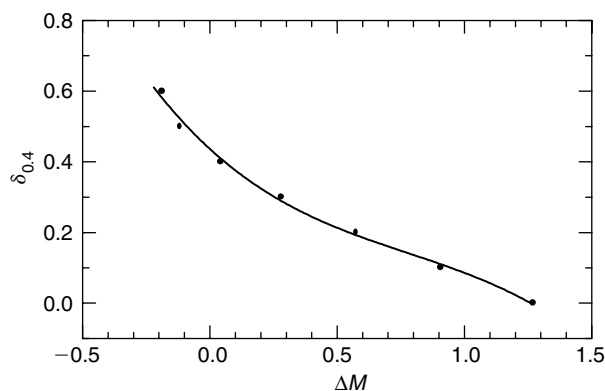


Figure 5 $\delta_{0.4}$ versus mean absolute magnitude difference $\langle \Delta M \rangle$.

UV-excess. However, as it can be seen from Figures 1 and 3, the offset from the fiducial main-sequence of Hyades behaves differently for different colour-index intervals, confirming the necessity of different equations for different $(B-V)_0$ intervals.

As admitted by LCL, they forced their calibration in order to pass through the zero point, thus supplying the Hyades absolute magnitudes for $\delta_{0.6} = 0$. In this study we have used the updated data (see Appendix) and have obtained a quadratic equation for the Hyades sequence. However, our calibration does not pass through the zero point either. Hence, we normalised the fiducial main-sequence of Hyades. This approach supplies absolute magnitudes almost equal to the Hyades absolute magnitudes for $\delta_{0.6} = 0$, for all $(B-V)_0$ intervals.

The comparison of the estimated absolute magnitudes with the original ones confirms the accuracy of our calibration. The mean of the differences of absolute magnitudes for each $(B-V)_0$ interval is almost zero and their standard deviations are only few percent (Table 5). The mean difference for stars with $0.3 < (B-V)_0 \leq 1.1$ and the corresponding standard deviation are $+0.0002$ and ± 0.0613 mag, respectively. Moreover, the plot of these differences versus the original absolute magnitudes shows that most of the stars lie within the interval $-0.1 < \Delta M(V) < +0.1$

(Figure 4a). Whereas the comparison of the absolute magnitudes estimated by LCL with the original ones gives larger means and standard deviations (Table 5). The mean difference and the corresponding mean standard deviation for all stars are -0.0151 and ± 0.4782 mag, respectively, rather different values than those from the new procedure. Finally, Figure 4b also demonstrates the large range of the absolute magnitude differences for LCL, i.e. the majority of stars lie within $-0.5 < \Delta M(V) < +0.5$ and there are about one hundred stars with still larger differences.

The colour-equations of Fukugita et al. (1996) provide a new metallicity calibration for the Sloan photometry. This has been carried out by the relation of normalised UV-excesses in the UBV and Sloan photometric systems, i.e. by substituting $\delta(U-B)_{0.6} = 0.725 \delta(g'-r')_{0.4}$ into the metallicity calibration of Karaali et al. (2003). The same substitution into equation (8) transforms the offset from the fiducial main-sequence of Hyades from UBV to Sloan photometry (equation 20) and finally the combination of (19) and (20) provides absolute magnitude estimation for the Sloan photometry.

We applied the new procedure to a set of artificial stars with $(g'-r')_0$ between 0.20 and 0.50, and compared the absolute magnitudes derived for seven different metallicities with the absolute magnitudes evaluated by means of the colour–magnitude diagram of M13. This is an example to see how coincident are the present approach and the canonical one. The mean of the differences between the absolute magnitudes derived by the new procedure and the canonical one is large for relatively metal-rich stars, is zero for the metallicity $[\text{Fe}/\text{H}] = -2.23$ dex and has a large range extending from $\langle \Delta M \rangle = 1.269$ to $\langle \Delta M \rangle = -0.186$. It is surprising that the coincidence occurs for the metallicity of M92 but not for the metallicity of M13 ($[\text{Fe}/\text{H}] = -1.4$ dex). One can argue that the metal-rich stars are not efficient in the deep surveys. However, the range of $\langle \Delta M \rangle$ extends from $+0.4$ to -0.2 even for the metallicity range from -1.0 to -3.0 dex, which is dominated by Population II stars. Additionally, the standard deviations (Table 9) for the seven comparisons mentioned above are larger than $\sigma = \pm 0.2$ mag, resulting in an

extra internal error in absolute magnitude estimation. The combination of these effects encourages us to claim that a single colour–magnitude diagram does not supply reliable absolute magnitudes for stars with a large range of metallicities. On the other hand, the small scattering of the differences between the original and the estimated absolute magnitudes for the UBV photometry confirms the significant improvement of the new procedure with respect to that of LCL. Finally, regarding the colour-equations of Fukugita et al. (1996), we argue that the new procedure can also be applied extensively and efficiently to SDSS (and to other systems, using appropriate colour-equations).

Accessory Materials

An Appendix detailing a Hyades sequence evolution and the raw data (Tables S1 and S2) are available as accessory material from PASA (www.csiro.au/journals/pasa/) or from the authors.

References

- Cameron, L. M. 1985, *AJ*, 146, 59
- Carney, B. W. 1979, *ApJ*, 233, 211
- Chen, B., Stoughton, C., Smith, J. A., Uomoto, A., Pier, J. R., Yanny, B., Ivezić, Z., York, D.G., Anderson, J. E., & Annis, J. 2001, *ApJ*, 553, 184
- ESA 1997, The Hipparcos and Tycho Catalogues, ESA SP-1200
- Fukugita, M., Ichikawa, T., Gunn, J. E., Doi, M., Shimasaku, K., & Schneider, D. P. 1996, *AJ*, 111, 1748
- Karaali, S., Bilir, S., Karatas, Y., & Ak, S. G. 2003, *PASA*, 20, 165
- Laird, J. B., Carney, B. W., & Latham, D. W. 1988, *AJ*, 95, 1843 (LCL)
- Nissen, P. E., & Schuster, W. J. 1991, *A&A*, 251, 457
- Perryman, M. A. C., Brown, A. G. A., Lebreton, Y., Gomez, A., Turon, C., de Strobel, G. Cayrel; Mermilliod, J. C., Robichon, N., Kovalevsky, J., Crifo, F. 1998, *A&A*, 331, 81
- Phleps, S., Meisenheimer, K., Fuchs, B., & Wolf, C. 2000, *A&A*, 356, 108
- Richer, H. B., & Fahlman, G. G. 1986, *ApJ*, 304, 273
- Ryan, S. G. 1989, *AJ*, 98, 1693
- Sandage, A. 1969, *ApJ*, 158, 1115
- Siegel, M. H., Majewski, S. R., Reid, I. N., & Thompson, I. B. 2002, *AJ*, 578, 151
- Yi, S., Demarque, P., Kim, Y., Lee, Y., Ree, C. H., Lejeune, T., Barnes, S. 2001, *ApJS*, 136, 417